# Axillary fat metastasis in breast cancer: A case report

SHILONG ZHANG[1*], JUAN CHEN[2*], YAN ZHANG[1*], ZHANGBO XU[1], JIECHAO REN[1], SIYANG HUANG[1], ZHUJUAN WU[1] and JIAN WU[1]

[1]Center of Breast and Thyroid Surgery, Department of General Surgery, The Third People's Hospital of Chengdu, Affiliated Hospital of Southwest Jiaotong University and The Second Affiliated Hospital of Chengdu, Chongqing Medical University, Chengdu, Sichuan 610031, P.R. China; [2]Department of Pathology, The Third People's Hospital of Chengdu, The Affiliated Hospital of Southwest Jiaotong University and The Second Affiliated Hospital of Chengdu, Chongqing Medical University, Chengdu, Sichuan 610031, P.R. China

Received February 18, 2025; Accepted June 13, 2025

DOI: 10.3892/ol.2025.15158

**Abstract.** Metastasis remains the primary cause of mortality for patients with breast cancer. Breast cancer metastasis primarily occurs through direct infiltration, the lymphatic system and hematogenous spread, with the axillary lymph nodes being the most common metastatic sites, followed by the lungs, bones, liver and brain. However, metastasis to adipose tissue in malignant tumors is exceedingly rare. The present case report comprehensively describes the clinical diagnosis and treatment of a 54-year-old woman with a malignant tumor in the left breast that metastasized to the left axillary fat tissue. Furthermore, a discussion of relevant studies on fat metastasis in malignant tumors is presented.

## Introduction

Breast cancer is the most prevalent malignant tumor and the second leading cause of cancer-related mortality among women worldwide (1,2). In 2022, breast cancer was diagnosed in ~2.3 million women and resulted in ~670,000 deaths (3).

Metastasis is the cause of >90% of breast cancer-related deaths, with the axillary lymph nodes being the most frequent metastatic sites. In advanced stages, breast cancer often metastasizes to organs such as the lungs, bones, liver and brain (4). These metastatic patterns are determined by the complex interplay between the intrinsic properties of tumor cells and the unique microenvironment of target organs. Key mechanisms include the following: i) Chemokine-receptor interactions, such as the C-X-C motif chemokine (CXC) ligand 12-CXC receptor 4 axis in bone metastasis (5); ii) hemodynamic factors that direct circulating tumor cells to organs with rich capillary networks (4); and iii) supportive microenvironments enriched with growth factors and extracellular matrix components (4). By contrast, adipose tissue presents multiple biological barriers to metastasis, including sparse vascularization, absence of critical adhesion molecules and a metabolically hostile environment characterized by hypoxia and acidosis. These barriers make it an unfavorable niche for tumor cell colonization and proliferation (6). Breast cancer metastasis to adipose tissue is occasionally observed in patients with advanced-stage disease and widespread hematogenous dissemination, usually accompanied by metastases to other organs. Isolated adipose tissue metastasis is extremely rare.

The present report describes a rare case of breast cancer metastasizing to the axillary fat tissue. The aim of this case study is to highlight the diagnostic challenges and clinical implications associated with such atypical metastatic patterns. By presenting this unusual case and reviewing the relevant literature, this case report seeks to improve awareness among clinicians, enhance diagnostic accuracy, and inform surgical and pathological assessment strategies for similar presentations in patients with breast cancer.

## Case report

*Case presentation.* A 54-year-old woman was admitted to The Third People's Hospital of Chengdu (Chengdu, China) in November 2024. The patient had noticed a lump in the left breast >6 months prior to admission, but delayed seeking medical care due to the absence of symptoms such as pain, skin irritation or nipple discharge. Upon admission, a comprehensive physical examination performed by the attending physician revealed a hard, poorly mobile mass measuring ~2 cm in diameter, which was palpated in the upper outer quadrant of the left breast. The mass was mildly adherent to the surrounding tissues. No significant lymphadenopathy was detected in the axilla or supraclavicular region. In addition, routine physical examinations of the cardiovascular, respiratory and abdominal systems revealed no abnormalities. The patient had no notable past medical history. Mammography revealed a high-density, irregularly shaped mass measuring

*Correspondence to:* Professor Jian Wu, Center of Breast and Thyroid Surgery, Department of General Surgery, The Third People's Hospital of Chengdu, Affiliated Hospital of Southwest Jiaotong University and The Second Affiliated Hospital of Chengdu, Chongqing Medical University, 82 Qinglong Street, Chengdu, Sichuan 610031, P.R. China
E-mail: wooj69@163.com

*Contributed equally

*Key words:* breast cancer, metastasis, axillary fat, fat microenvironment

~35x24 mm with spiculated margins and internal calcifications in the upper outer quadrant of the left breast (Fig. 1A). Moreover, MRI of the breast indicated a mass of ~20x18 mm in the upper outer quadrant of the left breast, with an irregular shape and spiculated margins. The lesion demonstrated low signal intensity on T1-weighted images, along with mixed signals on fat-saturated T2-weighted images and notable enhancement on contrast-enhanced images (Fig. 1B and C). Additionally, color Doppler breast ultrasound demonstrated a hypoechoic nodule measuring ~20x14 mm at the 2-3 o'clock position of the left breast and 4 cm from the papilla (Fig. 1D). After contrast injection, the lesion, measuring 35x17 mm in size, exhibited uneven high enhancement and prominent vascular structures (Fig. 1E). A core needle biopsy indicated invasive breast cancer in the left breast (Fig. S1A and B). Immunohistochemistry (IHC) results revealed that the biopsy sample cells were positive (30%) for Ki-67 (exceeding the 14% threshold), strongly positive (90%) for estrogen receptor (ER), moderately-to-strongly positive (30%) for progesterone receptor (PR) and negative (1+) for human epidermal growth factor receptor 2 (HER2) (Fig. S1C-F). The interpretation of the IHC results was based on the 2024 Guidelines of the Chinese Society of Clinical Oncology (CSCO) for Breast Cancer (7). Specifically, ER and PR were considered positive if ≥1% of tumor cell nuclei showed staining; HER2 expression was interpreted according to standard scoring criteria, with 0-1+ regarded as negative, 2+ as equivocal (requiring fluorescence *in situ* hybridization confirmation) and 3+ as positive; and Ki-67 was considered high if the proliferation index was ≥14%. Additional preoperative examinations, including chest and abdominal computed tomography (CT), cranial CT and a whole-body bone scan, demonstrated no evidence of distant metastasis or abnormalities. Serum tumor marker levels were also assessed and demonstrated to be within normal ranges: Carcinoembryonic antigen (CEA) was 2.64 ng/ml (reference value, <4.7 ng/ml) and cancer antigen 15-3 (CA15-3) was 18.9 U/ml (reference value, <26.2 U/ml). The initial diagnosis was left-sided breast cancer (luminal B type, c*T2N0M0, stage IIA) (7,8). The tumor measured >2 cm in diameter, with no clinically evident axillary lymph node involvement and no signs of distant metastasis, consistent with a clinical stage of IIA (cT2N0M0) (8). According to these findings, as well as the results of the immunohistochemical analysis, the tumor was classified as the luminal B molecular subtype (7).

In December 2024, the patient underwent a left axillary sentinel lymph node biopsy and left breast quadrant resection under general anesthesia. During surgery, sentinel lymph nodes and adjacent fatty tissue were excised and sent for intraoperative pathological analysis. Frozen sections, rather than fresh tissue, were used in accordance with standard intraoperative diagnostic protocols to enable rapid evaluation. Analysis of the frozen sections identified four sentinel lymph nodes from the left axilla, all of which were cancer-free. The left breast mass was subsequently excised and frozen section analysis was performed. The specimen was rapidly frozen using a cryostat, sectioned at 5-10 $\mu$m thickness, stained with hematoxylin and eosin (H&E), and immediately evaluated under a light microscope by a pathologist. The analysis confirmed invasive cancer. Tumor margins, consisting of the inner, outer, superior, inferior, basal and skin flap, were determined to be cancer-free. The surgical procedure was completed without complications and the patient had an uneventful recovery. Postoperative pathological analysis of the excised breast tissue confirmed invasive breast cancer (Fig. 2A and B). The histological grading of breast tumors was performed according to the Nottingham histological score system (9), which evaluates three morphological features: Tubule formation, nuclear pleomorphism and mitotic count. Each component is scored from 1-3, and the total score determines the grade as follows: Grade I/G1 (well-differentiated; score 3-5) in which tumors closely resemble normal breast tissue, are less proliferative and generally indicate a favorable prognosis; grade II/G2 (moderately differentiated; score 6-7), in which tumors exhibit intermediate levels of differentiation and prognosis; and grade III/G3 (poorly differentiated; score 8-9), in which tumors show marked atypia, high mitotic activity and aggressive clinical behavior with a worse prognosis. The cancer focus was classified as Nottingham grade II/G2 (total score 6). Postoperative pathological examination confirmed that the tumor measured 35x26x15 mm in size, based on gross inspection of the resected breast-conserving specimen (data not shown). Histological analysis further demonstrated the presence of neural invasion (Fig. S2A). IHC staining for CD34, a specific marker of vascular endothelial cells, was negative, further confirming the absence of lymphatic or vascular infiltration (Fig. S2B). Additionally, all surgical margins, including the 12, 3, 6 and 9 o'clock orientations and the deep (basal) and superficial (skin) margins, were negative for tumor involvement (Fig. S2C-H). These findings supported the completeness of the resection and the absence of microscopic residual disease. The IHC results demonstrated that the cells from the excised left breast tissue were positive (~30% in hot spots) for Ki-67, strongly positive (90%) for ER, moderately positive (30%) for PR and negative (1+) for HER2 (Fig. 2C-F). These results were interpreted according to the CSCO 2024 guidelines. Furthermore, pathological examination of the left axillary sentinel lymph nodes revealed four nodes with no evidence of metastasis. However, invasive ductal carcinoma was detected in the fatty tissue adjacent to one of the lymph nodes (Figs. 3A and S3). IHC analysis of the axillary sentinel lymph nodes and fatty tissue revealed positive staining for pan-cytokeratin in the fatty tissue, while no expression was observed in the lymph nodes (Fig. 3B). This finding confirmed tumor invasion into the axillary fat tissue rather than the lymph nodes. The tumor focus was classified as Nottingham grade I/G1 (9) (total score 5), with a size of ~3.3x1.9 mm. IHC showed that the fatty tissue cells were positive (5%) for Ki-67, strongly positive (90%) for ER, moderately positive (30%) for PR, and negative (1+) for HER2 (Fig. 3C-F). These IHC interpretations were also determined using CSCO 2024 criteria. Based on all the aforementioned findings, the postoperative diagnosis of the patient was a malignant tumor of the left breast (breast cancer, luminal B type, pT2N0Mx, stage IIA) and a secondary malignant tumor of the left axillary fat tissue (luminal A type) (7).

According to the 2024 CSCO Guidelines for Breast Cancer and the recommendations of the multidisciplinary team of The Third People's Hospital of Chengdu, a treatment plan comprising four cycles of postoperative chemotherapy using the docetaxel + cyclophosphamide regimen followed by breast-conserving radiotherapy and adjuvant therapy with an aromatase inhibitor (AI) was recommended. Currently, the patient has completed

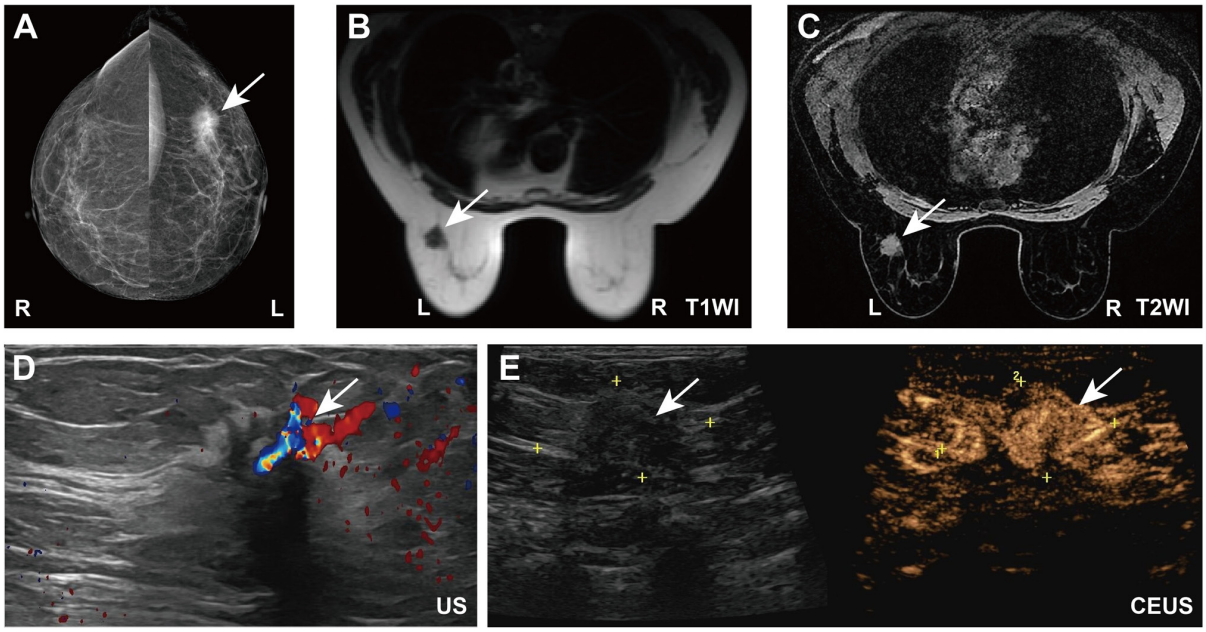


Figure 1. Preoperative imaging data of the patient. (A) Mammography. (B) T1- and (C) T2-weighted breast magnetic resonance imaging. (D) Actually color-Doppler ultrasound and (E) contrast-enhanced breast ultrasound of the patient before surgical treatment. White arrows indicate the location of the tumor. CEUS, contrast-enhanced ultrasound; WI, weight imaging.

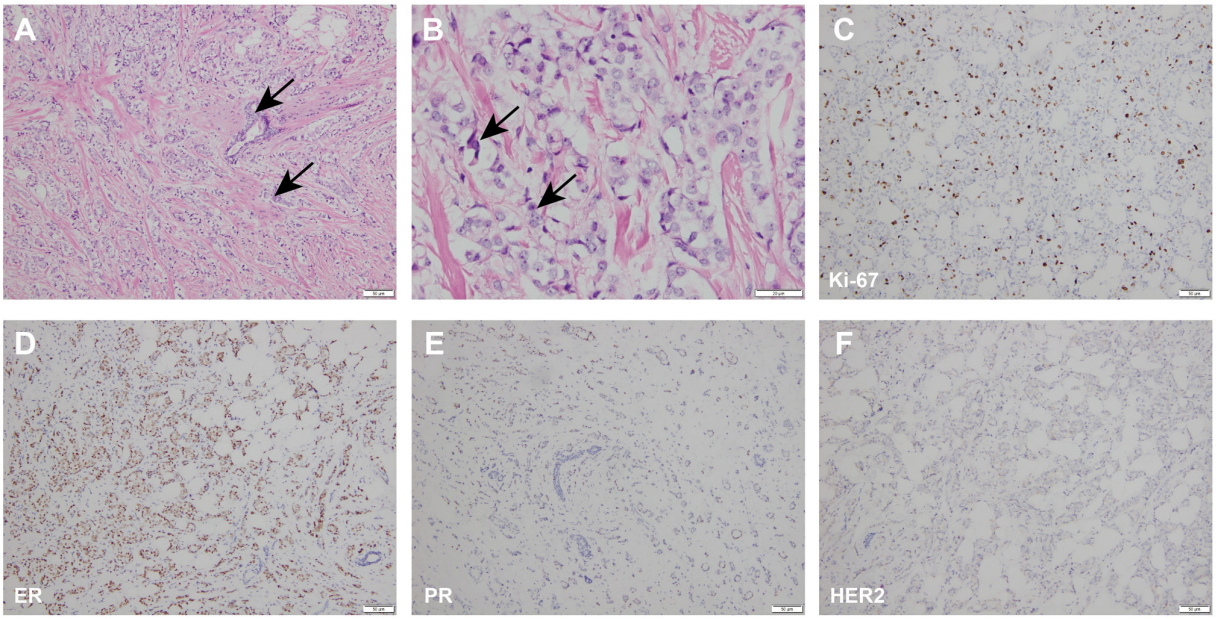


Figure 2. Pathological examination results of the left breast lumpectomy specimen. H&E staining at (A) x100 magnification (scale bar, 50 $\mu$m) and (B) x400 magnification (scale bar, 20 $\mu$m). Black arrows indicate tumor cells. IHC for (C) Ki-67 (magnification, x100; scale bar, 50 $\mu$m), (D) ER (magnification, x100; scale bar, 50 $\mu$m), (E) PR (magnification, x100; scale bar, 50 $\mu$m) and (F) HER2 (magnification, x100; scale bar, 50 $\mu$m) in the left breast lumpectomy specimen. IHC, immunohistochemistry; ER, estrogen receptor; PR, progesterone receptor; HER2, human epidermal growth factor receptor 2.

postoperative adjuvant chemotherapy (75 mg/m$^2$ of docetaxel + 600 mg/m$^2$ of cyclophosphamide, every 21 days as a cycle for a total of four cycles between December 2024 and March 2025). During chemotherapy, the patient experienced leukopenia, which improved following administration of lipegfilgrastim (6 mg). No other notable adverse events were observed. Breast-conserving postoperative radiotherapy was administered from April to May 2025. The regimen included whole-breast irradiation and coverage of the lymphatic drainage area of the left axilla, with a planned clinical target volume receiving 50 Gy in 25 fractions (2 Gy per fraction). This was followed by a sequential boost to the tumor bed, delivering an additional 10 Gy in 5 fractions (2 Gy per fraction). During radiotherapy, the patient developed mild erythema and swelling of the left breast and axilla, which resolved with topical burn ointment treatment. Following completion of chemotherapy in March 2025, the patient started adjuvant endocrine therapy with letrozole (2.5 mg every day) without any notable adverse effects to date.

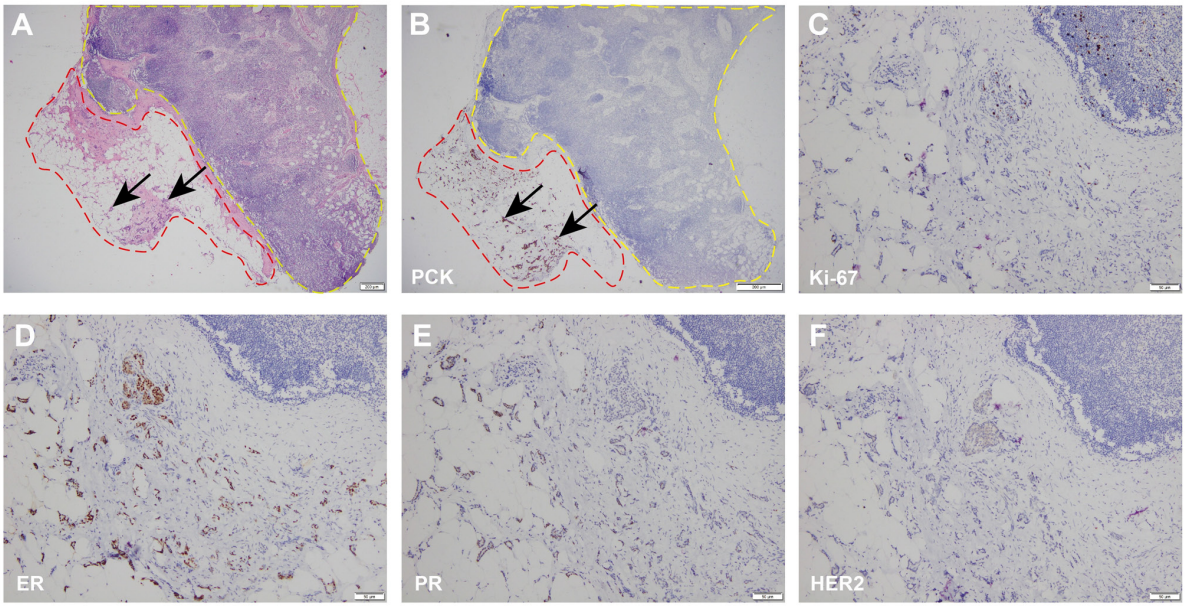


Figure 3. Pathological examination results of the left axillary sentinel lymph nodes and fatty tissue. (A) H&E staining at x20 magnification (scale bar, 200 $\mu$m). IHC for (B) PCK (magnification, x40; scale bar, 200 $\mu$m), (C) Ki-67 (magnification, x100; scale bar, 50 $\mu$m), (D) ER (magnification, x100; scale bar, 50 $\mu$m), (E) PR (magnification, x100; scale bar, 50 $\mu$m) and (F) HER2 (magnification, x100; scale bar, 50 $\mu$m) in the left axillary sentinel lymph nodes and fatty tissue. The yellow dashed box indicates the left axillary sentinel lymph node and the red dashed box indicates the adipose tissue adjacent to the left axillary sentinel lymph node (metastatic lesion). Black arrows indicate tumor cells. PCK, cytokeratin; ER, estrogen receptor; PR, progesterone receptor; HER2, human epidermal growth factor receptor 2.

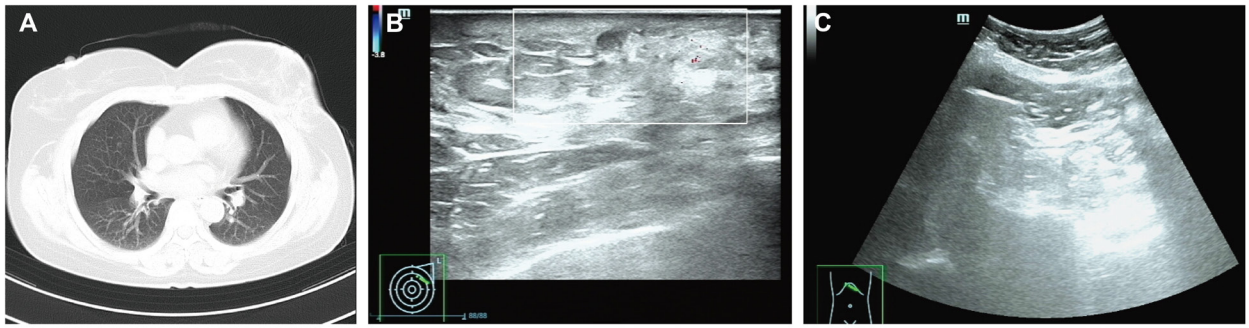


Figure 4. Radiological follow-up imaging of the patient. (A) Chest computed tomography showing no evidence of pulmonary or mediastinal metastasis. (B) Breast ultrasonography revealing postoperative changes in the left breast, with no signs of local recurrence. (C) Abdominal ultrasonography demonstrating no hepatic or peritoneal abnormalities.

Follow-up evaluations, including chest CT, breast and abdominal ultrasonography, and serum tumor marker assessments, have revealed no evidence of recurrence or metastasis as of May 2025. The most recent tumor marker levels were within the normal ranges as follows: CEA, 3.05 ng/ml (reference value, <4.7 ng/ml); and CA15-3, 19.6 U/ml (reference value, <26.2 U/ml). Radiological follow-up imaging in May 2025 also revealed no abnormal findings: Chest CT revealed no evidence of pulmonary or mediastinal metastasis (Fig. 4A), breast ultrasonography demonstrated postoperative changes in the left breast without signs of local recurrence (Fig. 4B) and abdominal ultrasonography was unremarkable, with no hepatic or peritoneal lesions identified (Fig. 4C). Furthermore, based on the 2024 CSCO Guidelines for Breast Cancer, the patient was recommended to continue AI-based endocrine therapy for 5 years. In addition, a structured follow-up surveillance plan was established, consisting of breast ultrasound every 3 months, and breast MRI and tumor marker evaluations every 6 months. This surveillance strategy aims to enable early detection of locoregional recurrence or distant metastasis, particularly given the unusual site of adipose tissue metastasis observed in the present case. Regular imaging and laboratory assessments are crucial for timely intervention and to improve long-term outcomes in patients with hormone receptor-positive breast cancer (7).

*H&E and IHC methods*. All histopathological and IHC staining procedures, including hematoxylin-eosin (H&E) and immunohistochemical staining, were performed by board-certified pathologists at the Department of Pathology at Chengdu Third People's Hospital.

*H&E method*. The biopsy specimens were fixed in 10% neutral buffered formalin at room temperature for 6-24 h. Tissue samples were then processed and embedded in

Table I. Full details of all antibodies.

| Antibody | Clone | Supplier | Cat. no. | Dilution |
|---|---|---|---|---|
| ER | SP1 | Roche Diagnostics | 05278406001 | RTU |
| PR | 1E2 | Roche Diagnostics | 05278392001 | RTU |
| HER2 | 4B5 | Roche Diagnostics | 05278368001 | RTU |
| Ki-67 | MIB-1 | Suzhou Bioda Medical Technology | PA451 | 1:100 |
| CD34 | QBEnd/10 | Suzhou Bioda Medical Technology | PA178 | 1:100 |
| PCK | AE1/AE3 | Suzhou Bioda Medical Technology | PA050 | 1:100 |

ER, estrogen receptor; PR, progesterone receptor; HER2, human epidermal growth factor receptor 2; PCK, pan-cytokeratin; RTU, ready-to-use.

paraffin. Sections were cut at a thickness of 4 $\mu$m, followed by H&E staining. Hematoxylin staining was performed for 5-10 min and eosin staining for 1-3 min, at room temperature. The stained slides were examined under a light microscope (Olympus BX43; Olympus Corporation).

*IHC method*. IHC was performed on formalin-fixed, paraffin-embedded tissue sections using the BOND-MAX Fully Automated immunostaining system (Leica Biosystems). First, tumor specimens were fixed in 3.7% neutral buffered formalin (Beijing Solarbio Science & Technology Co., Ltd.) for 24 h at room temperature, after which they were embedded in paraffin and sectioned into 4-$\mu$m thick slices. The sections were then mounted on positively charged slides and dried at 60˚C for 1 h. Subsequently, automated deparaffinization was performed using BOND Dewax Solution (Leica Biosystems), followed by heat-induced epitope retrieval with BOND Epitope Retrieval Solution 2 (EDTA-based, pH 9.0; Leica Biosystems) at 100˚C for 20 min. To block endogenous peroxidase activity, the slides were treated with 3% hydrogen peroxide (Leica Biosystems) for 5 min at room temperature. Non-specific binding was blocked with 10% normal goat serum (Wuhan Boster Biological Technology, Ltd.) for 20 min at room temperature. Subsequently, primary antibodies against ER, PR, HER2, Ki-67 and CD34 were applied. Detailed antibody information is listed in Table I. After 15 min of incubation at room temperature, sections were incubated with the secondary antibody from the BOND Polymer Refine Detection kit (cat. no. DS9800; Leica Biosystems), which includes an anti-mouse/rabbit HRP-conjugated polymer. Incubation was performed at room temperature for 8 min. DAB was used as the chromogen for visualization. Counterstaining was performed using hematoxylin for 5 min at room temperature, followed by dehydration and coverslip mounting. Finally, all stained slides were independently reviewed by two board-certified pathologists. In case of discrepancies, a joint re-evaluation was conducted until a consensus was reached. The results were interpreted according to the 2024 CSCO Guidelines for Breast Cancer, using standardized criteria for ER, PR, HER2 and Ki-67 positivity. Microscopic evaluation was performed using a standard light microscope (Olympus BX43; Olympus Corporation).

## Discussion

Tumor heterogeneity arises from the continuous genetic and epigenetic evolution of cancer cells during proliferation and progression. This dynamic process can lead to the emergence of subclonal populations with distinct molecular and biological characteristics, including differences in growth rate, invasiveness, therapeutic response and prognosis (10). In the present case, the primary lesion in the left breast was classified as Luminal B, whereas the metastatic lesion in the left axillary fat tissue exhibited a Luminal A profile. Luminal A breast cancers are typically characterized by high expression of ER, low expression of proliferation marker Ki-67, negative or low expression of HER2, and a generally favorable histological grade. These tumors are often less aggressive, have a lower risk of recurrence and respond well to endocrine therapy. By contrast, Luminal B tumors tend to show higher Ki-67 levels and lower PR expression, leading to a more aggressive clinical course and a comparatively worse prognosis (7). The discrepancy between the molecular subtypes of the primary and metastatic lesions in the present case underscores the spatial heterogeneity within the tumor and suggests the presence of distinct subclonal populations with different metastatic potentials. This heterogeneity highlights the complexity of breast cancer biology and poses notable challenges for diagnosis, prognostication and the development of personalized treatment strategies. In addition, pathological examination often reveals microscopic invasive foci or satellite nodules in the peritumoral region that are not readily detectable by imaging modalities. MRI primarily captures the main tumor mass and may underestimate the true extent of the lesion, especially when there is diffuse infiltration beyond the radiologically defined margins (11). In the present case, although both preoperative MRI and conventional breast ultrasonography suggested a tumor diameter of ~20 mm, other imaging techniques (such as mammography and contrast-enhanced ultrasound) were more consistent with the final pathological measurement of ~35 mm. Therefore, preoperative multimodal imaging evaluation serves a crucial role in accurately determining tumor size, staging and grading, and in guiding the selection of surgical approach. The diagnosis and treatment recommendations in the 2024 CSCO Guidelines for Breast Cancer are generally consistent with international standards such as the National Comprehensive Cancer Network (12) and the European Society for Medical Oncology (13); however, they also take into account regional clinical practices. For example, all guidelines advocate for the histopathological and immunohistochemical assessment of ER, PR, HER2 and Ki-67 status; however, the CSCO guidelines emphasize pragmatic and resource-sensitive

decision-making, especially when advanced genomic profiling (such as Oncotype DX and MammaPrint) is not readily available. With respect to endocrine therapy, AIs are recommended for postmenopausal women with hormone receptor-positive disease, in-line with international practices. Chemotherapy regimens may differ slightly due to population tolerability and accessibility of specific agents. Notably, in the present case, the postoperative follow-up plan, which consisted of regular physical examination, imaging and tumor marker evaluation, was based on an individualized risk-adapted strategy. By contrast, international guidelines typically advocate for less intensive routine surveillance in asymptomatic patients (7,12,13).

The ipsilateral axillary lymph nodes are widely recognized as the most common site of metastasis for breast cancer in the upper outer quadrant (14,15). Although the axillary fat tissue is anatomically adjacent to the breast, breast cancer metastasis exclusively to axillary adipose tissue without involvement of the sentinel lymph nodes or other common metastatic sites is extremely rare. However, intraoperative and postoperative pathological findings in the present case revealed no cancer cell infiltration in the sentinel lymph nodes within the axilla. Moreover, a small amount of invasive ductal carcinoma was found in the surrounding fatty tissue of one of the sentinel lymph nodes. During the review of the entire surgical process, the sentinel lymph nodes and adjacent fatty tissue were first excised for intraoperative pathological examination, followed by the completion of the left breast quadrant resection. Therefore, the possibilities of tumor seeding or implantation were not considered during surgery. Numerous solid tumors can extend into adjacent fatty tissue during their invasive process. For example, pancreatic cancer can invade the peripancreatic fat (16,17). Similarly, breast cancer with direct extension to subcutaneous or axillary fat tissue is theoretically possible yet rarely reported. The rarity of such presentations underscores the need for increased awareness and deeper mechanistic investigation. In the present case, no tumor cells were found in the adjacent breast fatty tissue following quadrant resection, whereas a small amount of invasive breast cancer was identified in the ipsilateral axillary fat tissue. This phenomenon of 'jump transfer' does not appear to have resulted from direct tumor infiltration. Previous studies emphasize that the fat microenvironment serves a critical role in the tumor microenvironment, particularly in the invasion of cancer types such as breast, ovarian and pancreatic cancer (18-20). Moreover, tumor cells can induce adipocyte dedifferentiation, which leads to adipocyte shrinkage, loss of lipid storage capacity and transformation into cancer-associated adipocytes (CAAs). These CAAs secrete several cytokines and chemokines that attract cancer cells and facilitate the formation of metastatic foci (21,22). CAAs also produce interleukin-6 and adipokines (leptin), which promote breast cancer cell proliferation and angiogenesis, and ultimately lead to breast cancer progression and metastasis (23). Additionally, recent studies have reported that CAAs can promote epithelial-mesenchymal transition in breast cancer cells by activating the CXCL12/AKT signaling pathway (24,25). Histologically, CAAs can be distinguished from normal adipocytes by several characteristic features, including reduced intracellular lipid content (resulting in smaller cytoplasmic vacuoles), a fibroblast-like or elongated cell shape, and their frequent localization adjacent to infiltrating tumor cells. Moreover, immunohistochemical markers such as perilipin-1 (with reduced or absent expression indicating adipocyte dedifferentiation), fatty acid binding protein 4 and leptin can assist in CAA identification; however, these markers are not routinely used in standard pathological evaluation (26,27). In the present case, formal detection of CAAs was not performed. However, the observed pattern of tumor infiltration into axillary fat, along with local adipocyte size variability, may suggest a reactive adipose microenvironment or early signs of adipocyte dedifferentiation. Therefore, further studies involving tissue-based profiling and functional assays are needed to validate the presence and role of CAAs in unusual metastatic patterns such as isolated axillary fat involvement.

Previous research has extensively investigated and elucidated hematogenous metastasis, lymphatic metastasis and metastasis to well-documented sites such as the bones, liver and lungs (28,29). However, metastasis of malignant tumors to adipose tissue is considered extremely rare in clinical oncology. Most reports describe direct invasion of adjacent fat by locally advanced tumors, whilst true distant metastasis to fat, particularly in the absence of involvement of common metastatic sites, is exceptionally uncommon (30). The current literature lacks large-scale epidemiological data on this phenomenon, and evidence is primarily derived from isolated case reports and small observational studies (31). The present report conducted a literature search using the PubMed database (https://pubmed.ncbi.nlm.nih.gov/) to identify reports of malignant tumors metastasizing to fatty tissue. The search was performed on February 20, 2025, and included publications from database inception to that date. The following search terms were used: ('cancer'[Title] AND ('fat'[All Fields] AND 'metastasis'[Title])) AND (case reports[Filter]). Only studies published in English and reporting human cases were included. Reviews, conference abstracts, animal studies and articles without full text were excluded. The search identified only one article specifically describing metastasis to fatty tissue in malignant tumors. In that study, abdominal CT identified a 17-mm nodule in the perirenal fat tissue of a 72-year-old male patient. Subsequent laparoscopic surgery and biopsy confirmed prostate cancer metastasizing to the perirenal fat (31). These findings suggest that fat metastasis is not an isolated or exceptional phenomenon and occurs more frequently than currently recognized. Therefore, heightened clinical awareness of fat metastasis is crucial, particularly in cases where traditional metastatic pathways do not fully explain the clinical presentation.

The present case report has several limitations. First, whilst the unique biological barriers of the adipose microenvironment that may contribute to the rarity of breast cancer metastasis to fat tissue are highlighted, the discussion remains largely descriptive. Due to the nature of a single-case clinical study, mechanistic investigations could not be performed, such as profiling of adipocyte-secreted cytokines, 3D co-culture models or single-cell RNA sequencing, to explore the molecular mechanisms underlying this metastatic behavior. Future studies incorporating *in vitro* or *in vivo* validation would be valuable in elucidating

the pathways involved and improving the understanding of this rare metastatic pattern. Second, PAM50 intrinsic subtyping, which could further stratify luminal subtypes and predict therapeutic responses with greater precision, was not performed in the present case. This limits the depth of molecular characterization and may impact the tailoring of individualized treatment strategies. Finally, due to the rarity of adipose metastasis and the single-institution nature of this report, no collaborative efforts with tertiary cancer centers were made to collect additional similar cases for comparative analysis. A larger cohort would allow for more comprehensive insights and strengthen the generalizability of the findings of the present report. Moreover, the follow-up period in this present case remains preliminary and does not fulfill the typical long-term follow-up standards suggested by the CARE guidelines (32). Further follow-up is essential to assess the durability of treatment response and to validate the long-term clinical relevance of this rare metastatic site.

In summary, to the best of our knowledge, the present study describes for the first time a rare case of breast cancer metastasizing to the axillary fat tissue, expanding the current understanding of atypical metastatic presentations in this malignancy. The results demonstrate that the identification of an axillary mass in patients with breast cancer should prompt clinicians to be vigilant and consider the possibility of fat metastasis. Lastly, comprehensive pathological examination remains the definitive method for characterizing such masses and distinguishing them from more common metastatic sites, such as the lymph nodes.

**Acknowledgements**

Not applicable.

**Funding**

Funding was received from The Third People's Hospital of Chengdu Clinical Research Program (grant no. CSY-YN-04-2025-007) and the China Foundation for Youth Entrepreneurship and Employment (grant no. P250308108823).

**Availability of data and materials**

The data generated in the present study are not publicly available due (compelling reason why data are not public) to but may be requested from the corresponding author.

**Authors' contributions**

SZ, JW, and YZ conceived and designed the study, and were the major contributors in writing the manuscript. JC performed the histological examination and contributed to manuscript writing. ZX, JR, SH, and ZW were responsible for data acquisition and made substantial contributions to data interpretation. SZ and JW confirm the authenticity of all the raw data. All authors read and approved the final manuscript.

**Ethics approval and consent to participate**

Not applicable.

**Patient consent for publication**

Written informed consent was obtained from the patient and their family for the publication of the present case report.

**Competing interests**

The authors declare that they have no competing interests.

**References**

1. Menon G, Alkabban FM and Ferguson T: Breast cancer. In: StatPearls. StatPearls Publishing, Treasure Island, FL, 2025.
2. Giaquinto AN, Sung H, Newman LA, Freedman RA, Smith RA, Star J, Jemal A and Siegel RL: Breast cancer statistics 2024. CA Cancer J Clin 74: 477-495, 2024.
3. Bray F, Laversanne M, Sung H, Ferlay J, Siegel RL, Soerjomataram I and Jemal A: Global cancer statistics 2022: GLOBOCAN estimates of incidence and mortality worldwide for 36 cancers in 185 countries. CA Cancer J Clin 74: 229-263, 2024.
4. Ibragimova MK, Tsyganov MM, Kravtsova EA, Tsydenova IA and Litviakov NV: Organ-specificity of breast cancer metastasis. Int J Mol Sci 24: 15625, 2023.
5. Worden AN, Pittard EG, Stern M, Uline MJ and Potts JD: The role of the CXCL12/CXCR4 signaling pathway in regulating cellular migration. Microsc Microanal 31: ozaf011, 2025.
6. Booth A, Magnuson A, Fouts J and Foster M: Adipose tissue, obesity and adipokines: Role in cancer promotion. Horm Mol Biol Clin Investig 21: 57-74, 2015.
7. Li J and Jiang Z: Chinese society of clinical oncology breast cancer (CSCO BC) guidelines in 2024: International contributions from China. Cancer Biol Med 21: 838-843, 2024.
8. Teichgraeber DC, Guirguis MS and Whitman GJ: Breast cancer staging: Updates in the AJCC cancer staging manual, 8th edition, and current challenges for radiologists, from the AJR special series on cancer staging. AJR Am J Roentgenol 217: 278-290, 2021.
9. Elston CW and Ellis IO: Pathological prognostic factors in breast cancer. I. The value of histological grade in breast cancer: Experience from a large study with long-term follow-up. Histopathology 19: 403-410, 1991.
10. Liu Q, Huang R, Jin X, Bai X, Tang W, Wang L, Karako K and Zhu W: Advances in research on receptor heterogeneity in breast cancer liver metastasis. Biosci Trends 19: 165-172, 2025.
11. Almahfouz Nasser S, Sharma A, Saraf A, Parulekar A, Haria P and Sethi A: Towards improving breast cancer detection through multi-modal image generation. Ultrasonics 153: 107655, 2025.
12. Etan T, Amir E, Tibau A, Yerushalmi R, Moore A, Shepshelovich D and Goldvaser H: National comprehensive cancer network recommendations for drugs without US food and drug administration approval in metastatic breast cancer: A cross-sectional study. Cancer Treat Rev 91: 102113, 2020.
13. Im SA, Gennari A, Park YH, Kim JH, Jiang ZF, Gupta S, Fadjari TH, Tamura K, Mastura MY, Abesamis-Tiambeng MLT, *et al*: Pan-Asian adapted ESMO clinical practice guidelines for the diagnosis, staging and treatment of patients with metastatic breast cancer. ESMO Open 8: 101541, 2023.
14. Leong SP, Pissas A, Scarato M, Gallon F, Pissas MH, Amore M, Wu M, Faries MB and Lund AW: The lymphatic system and sentinel lymph nodes: Conduit for cancer metastasis. Clin Exp Metastasis 39: 139-157, 2022.
15. Loi S, Michiels S, Adams S, Loibl S, Budczies J, Denkert C and Salgado R: The journey of tumor-infiltrating lymphocytes as a biomarker in breast cancer: Clinical utility in an era of checkpoint inhibition. Ann Oncol 32: 1236-1244, 2021.
16. Bai X, Wu L, Dai J, Wang K, Shi H, Lu Z, Ji G, Yu J and Xu Q: Rim enhancement and peripancreatic fat stranding in preoperative MDCT as predictors for occult metastasis in PDAC patients. Acad Radiol 30: 2954-2961, 2023.
17. Safi SA, Haeberle L, Rehders A, Fung S, Vaghiri S, Roderburg C, Luedde T, Ziayee F, Esposito I, Fluegen G and Knoefel WT: Neoadjuvant treatment lowers the risk of mesopancreatic fat infiltration and local recurrence in patients with pancreatic cancer. Cancers (Basel) 14: 68, 2021.

18. Zhu Q, Zhu Y, Hepler C, Zhang Q, Park J, Gliniak C, Henry GH, Crewe C, Bu D, Zhang Z, *et al*: Adipocyte mesenchymal transition contributes to mammary tumor progression. Cell Rep 40: 111362, 2022.
19. Maguire OA, Ackerman SE, Szwed SK, Maganti AV, Marchildon F, Huang X, Kramer DJ, Rosas-Villegas A, Gelfer RG, Turner LE, *et al*: Creatine-mediated crosstalk between adipocytes and cancer cells regulates obesity-driven breast cancer. Cell Metab 33: 499-512.e6, 2021.
20. Kothari C, Diorio C and Durocher F: The importance of breast adipose tissue in breast cancer. Int J Mol Sci 21: 5760, 2020.
21. Song Y, Na H, Lee SE, Kim YM, Moon J, Nam TW, Ji Y, Jin Y, Park JH, Cho SC, *et al*: Dysfunctional adipocytes promote tumor progression through YAP/TAZ-dependent cancer-associated adipocyte transformation. Nat Commun 15: 4052, 2024.
22. Wu Q, Li B, Li Z, Li J, Sun S and Sun S: Cancer-associated adipocytes: Key players in breast cancer progression. J Hematol Oncol 12: 95, 2019.
23. Yang Y, Ma X, Li Y, Jin L and Zhou X: The evolving tumor-associated adipose tissue microenvironment in breast cancer: From cancer initiation to metastatic outgrowth. Clin Transl Oncol 27: 2778-2788, 2025.
24. Dong Z, He L, Wu J, Xie C, Geng S, Wu J, Zhong C and Li X: Bisphenol A-induced cancer-associated adipocytes promotes breast carcinogenesis via CXCL12/AKT signaling. Mol Cell Endocrinol 599: 112473, 2025.
25. Olszańska J, Pietraszek-Gremplewicz K, Domagalski M and Nowak D: Mutual impact of adipocytes and colorectal cancer cells growing in co-culture conditions. Cell Commun Signal 21: 130, 2023.
26. Guo B, Wang K, Wu J, Yu H, Geng C, Jin Y and Song Y: Runx1 activates the transformation of adipocytes into cancer-associated adipocytes by downregulating Plin1. Exp Cell Res 448: 114573, 2025.
27. Guaita-Esteruelas S, Guma J, Masana L and Borràs J: The peritumoural adipose tissue microenvironment and cancer. The roles of fatty acid binding protein 4 and fatty acid binding protein 5. Mol Cell Endocrinol 462: 107-118, 2018.
28. Gradishar WJ, Moran MS, Abraham J, Abramson V, Aft R, Agnese D, Allison KH, Anderson B, Bailey J, Burstein HJ, *et al*: Breast cancer, version 3.2024, NCCN clinical practice guidelines in oncology. J Natl Compr Canc Netw 22: 331-357, 2024.
29. Park M, Kim D, Ko S, Kim A, Mo K and Yoon H: Breast cancer metastasis: Mechanisms and therapeutic implications. Int J Mol Sci 23: 6806, 2022.
30. Nieman KM, Romero IL, Van Houten B and Lengyel E: Adipose tissue and adipocytes support tumorigenesis and metastasis. Biochim Biophys Acta 1831: 1533-1541, 2013.
31. Wakita T, Yamanaka K, Yoshimura A, Fukae S, Yoshida T and Kishikawa H: Perirenal fat metastasis of prostate cancer. Urol Case Rep 39: 101778, 2021.
32. Anderson BO, Braun S, Carlson RW, Gralow JR, Lagios MD, Lehman C, Schwartsmann G and Vargas HI: Overview of breast health care guidelines for countries with limited resources. Breast J 9 (Suppl 2): S42-S50, 2003.